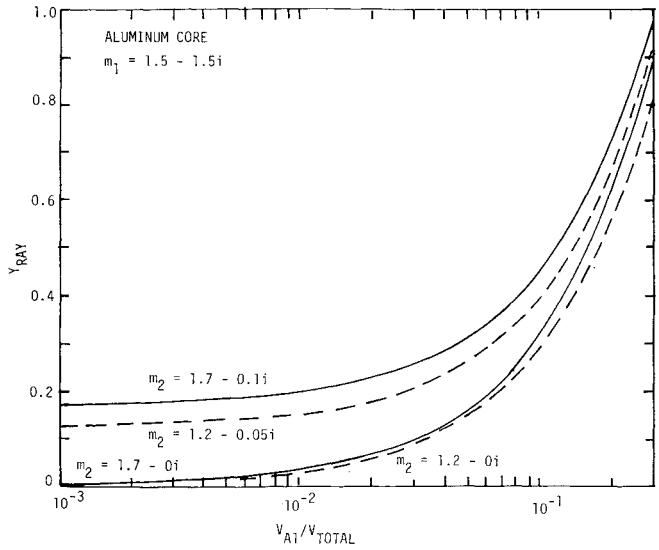

Fig. 1 Normalized alumina particle emissivity Y_{Ray} as a function of volume fraction of aluminum for a spherical particle with a spherical aluminum core and for several values of alumina complex index of refraction.

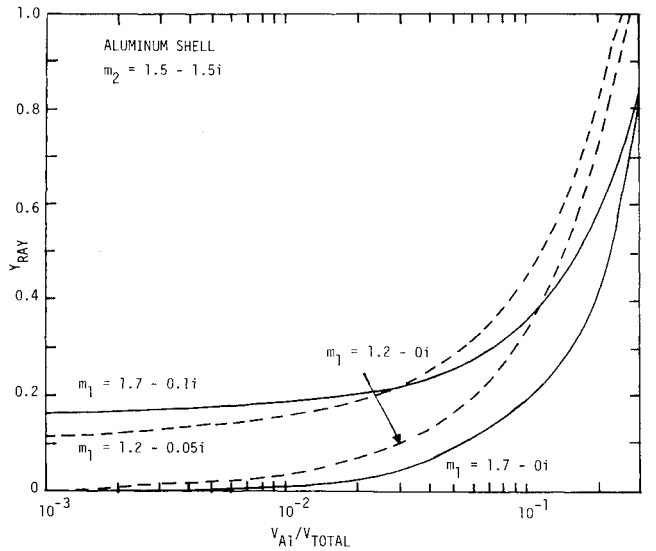

Fig. 2 Normalized alumina particle emissivity Y_{Ray}, as a function of volume fraction of aluminum for a spherical particle with a spherical shell of aluminum and for several values of alumina complex index of refraction.

Figure 1 shows the Rayleigh limit normalized emissivity Y_{Ray} for alumina particles with an unburned aluminum core. The emissivity is plotted against the ratio of volume of aluminum to total particle volume. The range of values of this ratio of primary interest here is up to 10^{-1} or so. The basic trend in the figure is that the emissivity increases as the amount of aluminum is increased. For particles containing a few percent metallic aluminum the enhancement of the emissivity is substantial, even for alumina which is by itself strongly absorbing (e.g., $m_{Al_2O_3} = 1.7 - 0.1i$). For an otherwise nonabsorbing particle (i.e., $k = 0$), a small aluminum core provides an emissivity large enough to provide a strongly radiating particle.

Figure 2 shows the emissivity for the opposite case of a thin metallic coating on the outside of an alumina sphere. The same trend is seen in this figure, viz., the emissivity increases as the amount of aluminum increases.

Conclusions

It is seen from the results presented here that small amounts of aluminum (on the order of a few percent by volume) lead to relatively large values for composite particle emissivities, even for cases in which the matrix material (i.e., alumina) is poorly absorbing by itself. These calculations were performed for the symmetric cases of a spherical core and a spherical shell and for the small-particle Rayleigh limit. Different values of alumina or aluminum complex index of refraction from those used in Figs. 1 and 2 lead to quite similar results.

Qualitatively, it would be expected that this behavior of emissivity enhancement would also exist in the Mie regime (particle radius ~ wavelength) and the bulk behavior regime (particle radius ≫ wavelength). In addition, it would be expected that the qualitative features of enhancement would also exist for composite particles of complex and nonsymmetric structure. In order to treat such particles quantitatively, a suitable nonsymmetric model would have to be constructed.

Clearly, small amounts of unburned aluminum contained in or on rocket exhaust alumina would go a long way toward explaining the discrepancies between measured pure alumina emissivity and the large amount of infrared particulate emission typically seen from aluminized solid-propellant rocket plumes.

Acknowledgments

This work was supported by Systems Control, Inc. with I.R. and D. funds.

References

[1] Worster, B., and Kadomiya, R., "Rocket Exhaust Aluminum Oxide Particle Properties," Aerodyne Research, Inc., Rept. No. ARI-RR-30, Aug. 1973.

[2] Rieger, T., Sepucha, R., and Fullerton, J., "IR Radiation from Low Altitude Rocket Exhausts. Documentation Report for the Computer Code ARC 1," Aerodyne Research, Inc., Rept. No. RR-66, May 1975.

[3] Gany, A., Caveny, L., and Summerfield, M., "Aluminized Solid Propellants Burning in a Rocket Motor Flowfield," *AIAA Journal*, Vol. 16, July 1978, pp. 736-739.

[4] Van de Hulst, H.C., *Light Scattering by Small Particles*, John Wiley and Sons, Inc., New York, 1957.

[5] Güttler, A., *Ann. Physik*, Vol. 6, Folge, Bde. 11, 1952, p. 65.

[6] Wickramasinghe, N., *Light Scattering Functions for Small Particles*, Adam Hilger, Ltd., London, 1973, p. 31.

Launch Window for a Shuttle-Based Geosynchronous Orbit Mission

W.H. Wright
Hughes Aircraft Co., El Segundo, Calif.

Introduction

IN launching geosynchronous orbit payloads there is a well-established sequence of events that proceeds from a low circular parking orbit to an elliptic transfer orbit with apogee near geosynchronous altitude and an inclination near 27 deg, and finally to the geosynchronous orbit with nearly zero inclination and eccentricity. During the transfer orbit phase the satellites are almost always spin-stabilized. Many

Received March 23, 1979; revision received May 15, 1979.

Index category: LV/M Mission Studies and Economics.
*Senior Scientist, Space and Communications Group.

payloads will be placed in orbit in this manner via the STS.[1] Two attitudes are defined – one for injection into the transfer orbit and another for firing the apogee motor to leave the transfer orbit for a nearly geosynchronous orbit. These attitudes each define a value of the sun aspect angle ϕ shown in Fig. 1 as the angle between the spin axis direction and the satellite/sun line. This angle determines the spacecraft thermal environment as well as its ability to generate solar power. Thus, it is found that the allowed range of ϕ is limited. This limitation defines a launch window, since for any given attitude the angle ϕ is determined by the time at which the launch vehicle lifts off. Generally the allowed range of ϕ is centered on 90 deg, giving the well-known result of launch windows near local noon and midnight at the point of injection. The same problem exists for STS launched satellites, but is made more complex by the flexibility of the orbital injection procedure from the shuttle. This is the problem to which this Note is addressed.

Opportunities for Injection into Transfer Orbit

The STS establishes itself in a 160-n.mi. circular parking orbit with an inclination of about 28.5 deg.[2] Transition from this parking orbit to a transfer orbit is effected by firing a perigee motor. This firing can take place at one of a number of equator crossings referred to as injection opportunities (IO). These opportunities are divided into ascending and descending node categories.

Corresponding to each of the ascending and descending node injection categories is an injection attitude, fixed in Earth coordinates, that will give the desired transfer orbit trajectory. Similarly there are two apogee motor firing (AMF) attitudes that will produce the desired drift orbit. While these attitudes are fixed in Earth coordinates, they vary in inertial space. One component of this variability arises from varying STS liftoff time which means that the same IO occurs at a different point in inertial space. Another component stems from the roughly 7.5deg/day regression of the parking orbit nodal right ascension. Thus, after liftoff, each IO has a unique inertial attitude associated with it. The changing attitudes represent varying values of the sun aspect angle ϕ, which must lie in the 90 deg $\pm$ 25 deg range. There is an additional variation in this angle that is independent of attitude and is produced by the Earth's motion around the sun. This results in an effective 1 deg/day motion of the sun in the Earth-centered inertial system.

Since injection into both transfer and drift orbits takes place at or near equator crossing, there are very specific Earth-fixed attitudes that are acceptable. When these are combined with the allowed sun angle range, there are generally two bands of time, close to local (in this case near GMT) noon and midnight, during which the STS can lift off. If these opportunities are viewed in inertial space, as in Fig. 2, it is seen that both midnight and noon injections are possible for both midnight and noon launches. Thus, for a midnight launch the odd numbered IO's are near local midnight, the even numbered IO's near local noon. It is seen that nodal regression separates successive odd (or successive even) IO's by about 0.47 deg in inertial space. This regression of the node limits the number of IO's satisfying the ϕ constraint.

Ejection of the payload from the STS takes place only after parking orbit is achieved. The subsequent 45-min coast phase between ejection and injection eliminates at least IO's 1, 2, and 3 from consideration. After injection tracking, telemetry, and command (TT&C) stations must acquire and track the spacecraft in order to collect data and transmit commands. Generally, from 3 to 7 passes, each lasting up to 9 h are required to perform the transfer orbit mission. Simulation has shown that there are many IO's that meet this condition. If the Canadian satellite ANIK C, together with the Telesat Canada ground network of TT&C stations at Allan Park, Ont., Lake Cowichan, B.C., and Guam, is taken as a typical case, it is found that there are more than 120 possible IO's, and of this number approximately 25% provide ample opportunity for orbit and attitude determination and maneuvers.

It is operationally convenient to choose a specific IO with a limited range of acceptable IO's about it for backup, and to confine launch window analysis to this range of IO's. Because of the sufficiency and distribution of adequate opportunities there should generally be no problem in obtaining a favorable IO range, even when STS operational constraints (as yet not

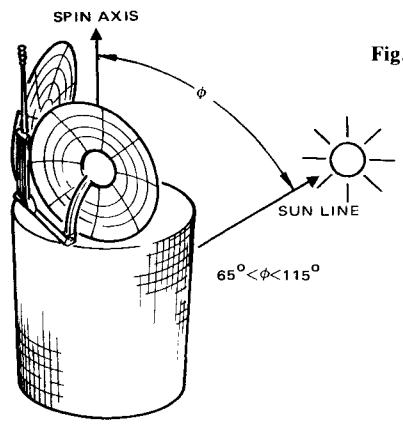

Fig. 1 Sun angle constraint.

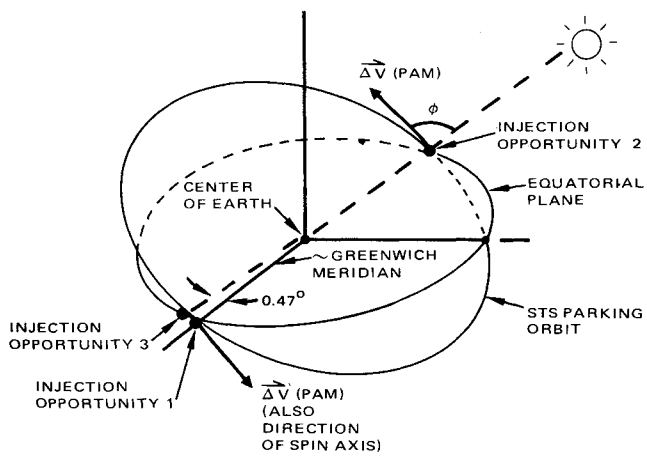

Fig. 2 Midnight launch injection opportunities viewed in inertial space.

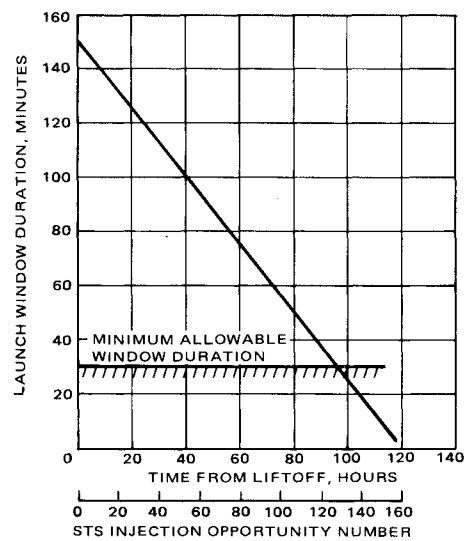

Fig. 3 STS midnight launch window for midnight injections 1 to 13.

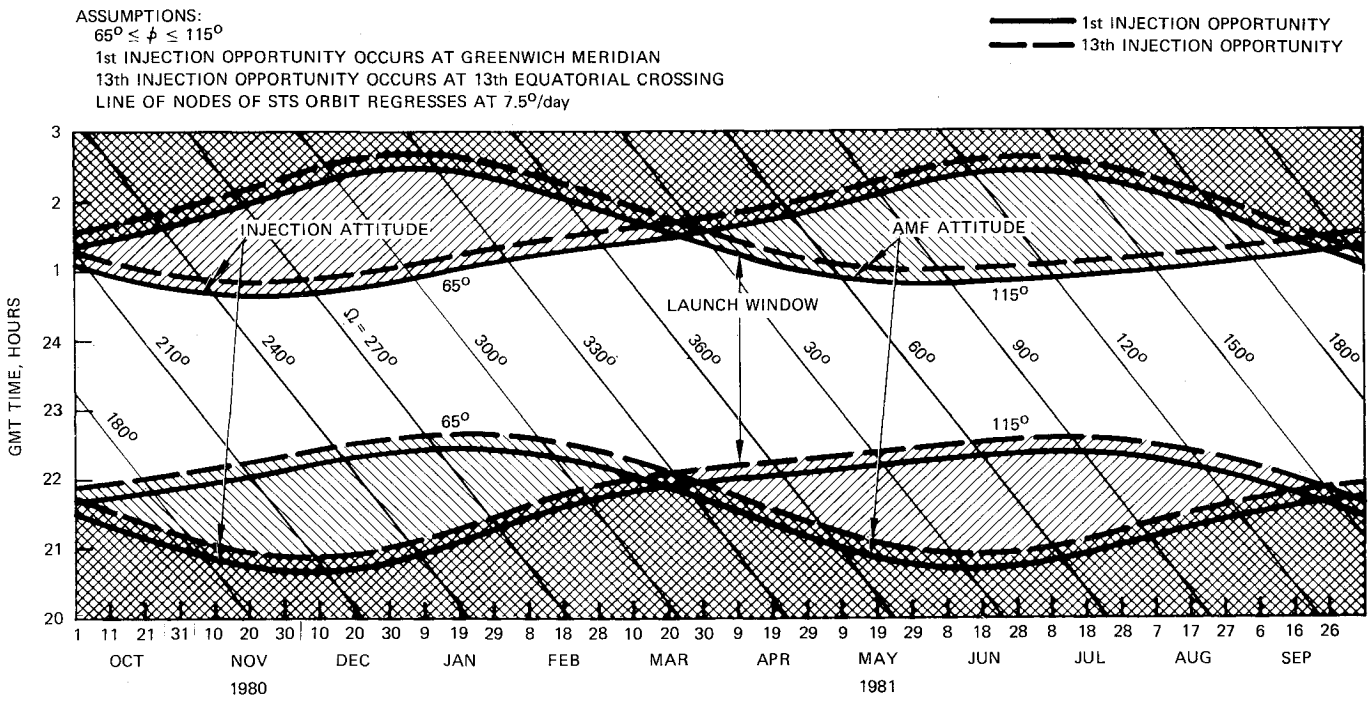

Fig. 4 Launch window duration vs time for STS liftoff.

fully defined) are imposed. This range of IO's defines an injection window (as distinct from a launch window), a concept that is useful since it stipulates the boundaries of injection in terms of time.

Launch Window and Additional Constraints

Midnight launch windows for IO's 1 and 13 are shown in Fig. 3 for Oct. 1, 1980 to Sept. 30, 1981. In generating these curves a sun angle range of $\phi = 90$ deg ± 25 deg was assumed, and it was further assumed that the first equatorial crossing (IO 1) takes place on the Geenwich meridian. It is evident from Fig. 3 that the launch window is reduced as more opportunities are included in the analysis. The window duration as a function of IO number is shown in Fig. 4, where it is seen that within four days of liftoff the window is less than the generally required minimum of 30 min. This effect results principally from nodal regression in the STS parking orbit, which causes the required injection and AMF $\Delta\bar{V}$'s to rotate, thereby changing the sun aspect angle ϕ.

For many of the spacecraft launched into geosynchronous orbit there is a 30-min limitation on the time that can be spent in eclipse per transfer orbit. This becomes an additional constraint in defining the launch window. The expected duration of these eclipses is a nearly constant 23 min for midnight injection, since eclipse occurs near perigee. Noon IO's have longer eclipse periods of up to approximately 140 min near the equinoxes. There are, however, times of the year when the noon injection is eclipse-free. If the launch date is removed from an equinox by more than 25 days, for instance, there is no eclipsing for injection right at noon. It is important to realize that long transfer orbit eclipses can occur even for a midnight launch. The governing factor is the time of injection, not of launch, so it is the noon injection that is constrained and not necessarily the noon launch.

Conclusions

STS launched geosynchronous orbit payloads that are spin stabilized in their transfer orbits will be subject to restrictions on the time of day at which liftoff can occur. As with expendable booster launches, these times are near noon and midnight at the point at which injection into transfer orbit takes place. But there now are many opportunities to inject into this orbit from the 160-n.mi. STS parking orbit. The total number of these IO's is limited by dal regression in the parking orbit; however, a more practical limit is imposed by the nominal 3-day duration of STS missions. Since both ascending and descending node injections can be considered, there are two, rather than one, Earth-fixed attitudes for each of the injection and AMF events. For planning purposes a range of IO's will be selected for each payload leading in addition to the launch window, to an injection window.

Acknowledgments

The author is grateful for the programming assistance of B. Wandzura and the helpful suggestions of M. Neufeld and D. Horton.

References

[1]Teasdale, W.E., "Space Shuttle Payloads and Data Handling Accommodations," *IEEE Transactions on Communications*, Vol. 26, Nov. 1978, pp. 1557-1567.

[2]Schiesser, E.R., "Use of Radio Equipment for Space Shuttle Navigation," *IEEE Transactions on Communications*, Vol. 26, Nov. 1978, pp. 1514-1520.

Growth of HgI_2 Single Crystals in Spacelab III

W.F. Schnepple,* L. van den Berg,† and N. Skinner‡
EG&G, Santa Barbara Operations, Goleta, Calif.

Introduction

MERCURIC iodide has been under development as a material for x- and gamma-ray detectors since approximately 1972. The main advantages of the material are

Presented as Paper 79-0307 at the 17th Aerospace Sciences Meeting, New Orleans, La., Jan. 15-17, 1979; submitted June 5, 1979; revision received Aug. 21, 1979.

Index category: Space Processing.

*Section Head III, Applied Science Dept.
†Scientific Specialist.
‡Technologist.